AD-A191 325 A NEW FIBER-OPTIC-BASED PHASE-RESOLVED PHOSPHORESCENCE SPECTROMETER(U) INDIANA UNIV AT BLOOMINGTON DEPT OF CHEMISTRY F V BRIGHT ET AL. 15 FEB 88 1/1

UNCLASSIFIED INDU/DC/GMH/TR-88-20 N00014-86-K-0366 F/G 20/6 NL

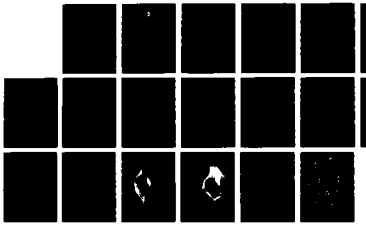

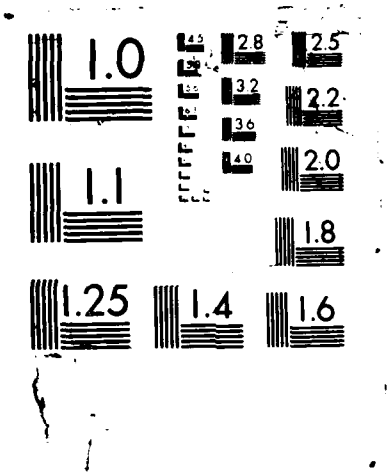
1.0
1.1
1.25
1.4
1.6
1.8
2.0
2.2
2.5
2.8
3.2
3.6
4.0

UNCLASSIFIED

SECURITY CLASSIFICATION OF THIS PAGE

(4)

DTIC FILE COPY

REPORT DOCUMENTATION PAGE

DTIC ELECTE FEB 24 1988 D

AD-A191 325

	1b. RESTRICTIVE MARKINGS: NA
	3. DISTRIBUTION/AVAILABILITY OF REPORT: Distribution Unlimited; Approved for Public Release
4. PERFORMING ORGANIZATION REPORT NUMBER(S): INDU/DC/GMH/TR-88-20	5. MONITORING ORGANIZATION REPORT NUMBER(S): NA
6a. NAME OF PERFORMING ORGANIZATION: Indiana University; 6b. OFFICE SYMBOL (If applicable): NA	7a. NAME OF MONITORING ORGANIZATION: ONR
6c. ADDRESS (City, State, and ZIP Code): Department of Chemistry, Bloomington, IN 47405	7b. ADDRESS (City, State, and ZIP Code): 800 N. Quincy Street, Arlington, VA 22217
8a. NAME OF FUNDING/SPONSORING ORGANIZATION; 8b. OFFICE SYMBOL (If applicable)	9. PROCUREMENT INSTRUMENT IDENTIFICATION NUMBER: Contract N00014-86-K-0366
8c. ADDRESS (City, State, and ZIP Code)	10. SOURCE OF FUNDING NUMBERS: PROGRAM ELEMENT NO.; PROJECT NO.; TASK NO. R&T Code 4134006; WORK UNIT ACCESSION NO.

11. TITLE (Include Security Classification)
A New Fiber-Optic-Based Phase-Resolved Phosphorescence Spectrometer

12. PERSONAL AUTHOR(S)
Frank V. Bright, Curtis A. Monnig, and Gary M. Hieftje

13a. TYPE OF REPORT	13b. TIME COVERED	14. DATE OF REPORT (Year, Month, Day)	15. PAGE COUNT
Technical	FROM ____ TO ____	15 February 1988	31

16. SUPPLEMENTARY NOTATION
Chapter to be published in Multidimensional Luminescence, ed. Isiah M. Warner, JAI Press.

17. COSATI CODES		
FIELD	GROUP	SUB-GROUP

18. SUBJECT TERMS (Continue on reverse if necessary and identify by block number)
Fiber optics; Sensors; Time-resolved luminescence; Phosphorimetry.

19. ABSTRACT (Continue on reverse if necessary and identify by block number)

A new phase-resolved phosphorescence spectrometer is described which employs a cw ultraviolet argon-ion laser as an excitation source. The excitation and phosphorescence radiation is carried to and from the sample through inexpensive optical fibers. Typical detection limits are less than 85 nM for all of the lumiphores studied. The new instrument is shown to be applicable to the simultaneous determination of the individual components in binary and ternary mixtures. In addition, the new instrument is used for the generation of multidimensional data sets. Specifically, the phase-resolved phosphorescence intensity vs. detector phase angle setting are collected rapidly (< 10 minutes) for several of the lumiphores studied. These multidimensional data arrays are subsequently used for multicomponent analyses.

20. DISTRIBUTION/AVAILABILITY OF ABSTRACT: ☒ UNCLASSIFIED/UNLIMITED ☐ SAME AS RPT ☐ DTIC USERS	21. ABSTRACT SECURITY CLASSIFICATION: Distribution Unlimited
22a. NAME OF RESPONSIBLE INDIVIDUAL: Gary M. Hieftje	22b. TELEPHONE (Include Area Code): (812) 335-2189; 22c. OFFICE SYMBOL

DD FORM 1473, 84 MAR 83 APR edition may be used until exhausted. All other editions are obsolete

SECURITY CLASSIFICATION OF THIS PAGE

UNCLASSIFIED

OFFICE OF NAVAL RESEARCH

Contract N14-86-K-0366

R&T Code 4134006

TECHNICAL REPORT NO. 20

A NEW FIBER-OPTIC-BASED PHASE-RESOLVED PHOSPHORESCENCE SPECTROMETER

by

Frank V. Bright, Curtis A. Monnig, and Gary M. Hieftje

Prepared for Publication

in

Multidimensional Luminescence
ed., Isiah M. Warner, JAI Press

Indiana University
Department of Chemistry
Bloomington, Indiana 47405

15 February 1988

ABSTRACT

A new phase-resolved phosphorescence spectrometer is described which employs a cw ultraviolet argon-ion laser as an excitation source. The excitation and phosphorescence radiation is carried to and from the sample through inexpensive optical fibers. Typical detection limits are less than 85 nM for all of the lumiphores studied. The new instrument is shown to be applicable to the simultaneous determination of the individual components in binary and ternary mixtures. In addition, the new instrument is used for the generation of multidimensional data sets. Specifically, the phase-resolved phosphorescence intensity vs. emission wavelength vs. detector phase angle setting are collected rapidly (< 10 minutes) for several of the lumiphores studied. These multidimensional data arrays are subsequently used for multicomponent analyses.

INTRODUCTION

The first reported observation of low-temperature phosphorescence was by Wiedmann in 1888 (1). In the following century Lewis and Kasha established that phosphorescence occurs from the triplet state and that its excited-state lifetime is significantly longer than that of fluorescence (2). The first analytical application of phosphorescence was reported by Keirs et al. (3) more than a decade after Lewis and Kasha published their findings. In general, the phosphorescence spectrum is much less vibrationally structured than the fluorescence spectrum for the same molecule. Because the phosphorescence spectra of numerous lumiphores are very similar, Winefordner and coworkers explored temporal resolution as an analytical selectivity parameter (4-10).

Luminescence lifetimes can be determined not only in the time domain; in fact, they were first determined in the frequency domain by Gaviola (11). Following excitation with sinusoidally modulated light, the resulting luminescence is equal in frequency, but phase shifted and amplitude demodulated to an extent which depends on the luminescence lifetime. Veselova et al. (12) developed a new frequency-domain technique, phase-resolved fluorescence spectroscopy, which resolves components based solely on their respective phase shifts. With phase-sensitive detection, the individual-component spectra of binary mixtures were resolved (12). Mousa and Winefordner were the first to employ phase-resolved measurements to phosphorimetry (13). Most recently, McGown and coworkers have explored the analytical application of phase-resolved fluorescence spectroscopy for simultaneous resolution of up to six components (14-22).

In the present paper we describe a new fiber-optic-based phase-resolved phosphorescence spectrometer and have evaluated it for the resolution of binary and ternary mixtures of several common lumiphores. Several areas were explored with the new instrument. First, it was shown that fiber-optic sensors could be conveniently employed for low-temperature (77 K) phosphorescence measurements. These findings support the initial work of Heiman, who employed fiber-optic sensors at temperatures down to 4K (23) and who first noted such measurements. Secondly, data-regression schemes similar to those described by McGown and coworkers (14-22) and Bright (24) were used successfully to resolve the individual components of lumiphore mixtures. Third, detection limits were evaluated. Finally, the advantages and disadvantages of this new instrument were compared to those of instruments described previously. These advantages include simplified optical alignment, high light-collection efficiency, the lack or need for a

quartz Dewar or focusing optics, elimination of interference from bubbles of boiling cryogenic fluid, compactness, low cost, and sampling versatility.

EXPERIMENTAL

Phase-Resolved Phosphorescence Spectrometer. Figure 1 shows a schematic diagram of the new fiber-optic-based phase-resolved phosphorescence spectrometer. All optical components were rigidly mounted on a 1.3m x 3m air-suspension optical table (Newport Research Co.). A cw argon-ion laser (model 171, Spectra Physics, Inc.) served as the excitation source, and was operated in the UV "all-lines" configuration at an average output power of up to 500 mW. The output of the laser was sinusoidally modulated in the 0.5-1000 Hz range by means of the signal from a function generator (model 1600, Krohn-Hite, Inc.) applied to the light-control input of the laser power supply. The depth of modulation was variable and depended on the modulation frequency employed, but in all cases was in excess of 15% and approached 100% below 30 Hz. Mirrors M1 and M2 (model 10QM20EM.35, Newport Research Co.) were used to direct the laser output to a Suprasil focusing lens (L_1; f.l.=10 cm) and from there into one arm of an optical fiber positioned on a fine-adjustment x,y,z translation stage.

The optical-fiber sensor (OFS, Figure 2) consisted of two identical 2.0-m segments of 200-μm diameter UV-grade cladded-multimode fiber (Galileo Fiber Optics, Inc.). The two segments of the OFS were epoxied (Epotek 320) together at the distal end in a 3-mm-diameter glass capillary. The glass capillary was then inserted through the screw cap of a micro sample vial (cat. no. B7782-1, 15mm x 45mm, American Scientific Products) and held in place, as shown in Figure 2, by two o-rings. At the distal end of the fiber the sample vial was placed on the screw cap (Figure 2), so the fiber was

covered by the sample to a depth of at least 1 cm. The entire vial and fiber assembly was then immersed directly into the cryogent (liquid nitrogen).

Luminescence (fluorescence and phosphorescence) radiation was collected by a second optical fiber whose output end was ridigly mounted in a stationary fiber-optic mount (FM, Figure 1). The radiation from this fiber was then focused by a glass lens (L_2; f.l.=20 cm) into a double monochromator (model 1680 Spectramate, Spex, Inc.) with a 9.0 nm spectral bandpass. Because all of the lumiphores that were studied exhibited emission in the visible portion of the spectrum, a UV-transmitting lens was not necessary in the emission channel. Detection of the resulting luminescence was achieved with a photomultiplier (model R928, Hamamatsu, Inc.) operated at a biasing voltage of -1350 V dc.

Phase-resolved detection (Figure 1) was achieved by connecting the output from the photomultiplier to a fast current amplifier (model 427, Keithley, Inc.) and from there to a phase-sensitive detector. The phase-sensitive detector is a simple lock-in amplifier (model 840 Keithley, Inc.) which is referenced to the laser modulation frequency through the function generator's TTL output.

Both the ac and dc (steady-state) components of the luminescence are required for the determination of the luminescence lifetimes by the demodulation method (25-30). For dc detection, the output from the photomultiplier was simply connected to a picoammeter (model 414S, Keithley, Inc.) and the dc level recorded by a digital voltmeter (model 8024A, Fluke, Inc.). To record the ac signal, the photomultiplier output was connected to one input of a two-channel digital storage oscilloscope (model 3091, Nicolet, Inc.) referenced to the modulation waveform through an external

photodiode. The photodfode was used only to monitor the laser's original modulation waveform. The output from this photodiode was then input to the second channel of the digital oscilloscope. The two traces (luminescence and photodiode response), when stored on the oscilloscope screen, provide a simple positional reference for the phase-shift measurement also. The entire data collection was interactively controlled by a computer (model MINC 11/23, Digital Equipment Corp.). All data regression was performed using an Apple IIe microcomputer employing least-squares programs described elsewhere (24).

Reagents and Materials. Anthracene, acridine, phenazine, 7,8-benzoquinoline, and 5,6-benzoquinoline were all purchased commercially (Aldrich Chemical Co.). m-Nitrophenol was purchased from Fisher Scientific and p-nitrophenol acquired from MCB Reagents. Liquid nitrogen was used as the cryogent for all phosphorescence measurements. A 1.00 mM stock solution of each lumiphore was prepared in absolute ethanol (AAPER Alcohol & Chemical Co.) and sonicated for 30 minutes to insure complete mixing. Synthetic samples were all prepared in absolute ethanol and no steps were taken to further degas the samples (31). Upon freezing, each sample decreased in volume to about 75% of its original value. All concentrations are quoted for the samples at room temperature.

General Operation

Luminescence (Phosphorescence) Lifetime Determinations. While scattered radiation from a reflective aluminum surface was monitored, the waveform from the reference photodiode and photomultiplier were simultaneously stored on the digital oscilloscope and sent to the phase-sensitive detector. The

phase-shift and amplitude ratio between these two waveforms then served as the reference phase shift (ϕ_R) and modulation factor (m_R) for the exciting radiation, respectively (25-27). Ideally, these values represent also the phase shift and modulation factor at the appropriate emission wavelength. However, it has been shown that photomultipliers exhibit a wavelength-dependent temporal response as high as 100 ps/10 nm (32). For the faster fluorescence phenomenon this error is significant, but for the longer-lived phosphorescence the effect is negligible and has been ignored here.

Following the determination of ϕ_R and m_R, a sample vial is "mounted" onto the optical-fiber sensor (Figure 2). The sample and fiber are then completely immersed into a Dewar containing liquid nitrogen; the sample is frozen solid in about one minute. For best results a clear glass should be employed; if a fractured sample is produced, one simply needs to thaw and refreeze the solution. The desired emission wavelength is then selected by the monochromator and the resulting waveform from the photodiode and photomultiplier are again simultaneously stored and recorded by the digital oscilloscope and lock-in amplifier. The difference between these two waveforms is the observed phase shift (ϕ_0) and modulation factor (m_0), respectively, for the phosphorescence (28-30). From this set of measurements (ϕ_R, ϕ_0, m_R, and m_0), the observed phosphorescence lifetime is calculated from the shift (ϕ) as (13):

$$\tau = \frac{1}{\omega} \tan \phi \qquad (1)$$

or from the demodulation factor (M):

$$\tau = \frac{1}{\omega} \left(\frac{1}{M^2} - 1 \right)^{1/2} \qquad (2)$$

where ω is the angular modulation frequency ($\omega = 2\pi f$, f=linear modulation frequency; Hz) and ϕ and M are given by:

$$\phi = \phi_O - \phi_R \tag{3a}$$

$$M = \frac{m_O}{m_R} \tag{3b}$$

This measurement procedure is repeated at a number of selected modulation frequencies until the entire ϕ vs. f and M vs. f curves have been generated. This procedure is analogous to the approaches used in multifrequency amplitude (28) or phase (29,30) fluorimetry. Of course, a luminescence lifetime can be calculated at a single modulation frequency, but the complexity of the decay process cannot be studied unless several modulation frequencies are employed (33). For twenty modulation frequencies over the 0.5-1000 Hz range and at a single emission wavelength, this entire procedure takes approximately one hour to complete. The rich information content of such data can reveal the number of different emitting species in a sample and the fractional contribution of each to the total luminescence signal (25-30,34,35).

Phase-Resolved Phosphorescence: Spectral Acquisition. Before the samples are frozen, the phase of the lock-in amplifier is adjusted to nullify the fluorescence contribution from the samples. Afterward, the recorded emission is due only to phosphorescence (13). For most of the samples that were studied, the fluorescence intensity decreased slightly upon freezing of the solution, and the phosphorescence signal correspondingly increased.

Phase-Resolved Phosphorescence: Component Resolution. The procedure and theoretical considerations of quantitative multicomponent resolution using phase-resolved techniques have been described in detail elsewhere (21,24). Briefly, a series of single-component standard solutions was employed and the dependence of the phase-resolved phosphorescence intensity (PRPI) on detector phase angle (lock-in amplifier phase setting) was measured as a function of emission wavelength. Multicomponent sample mixtures were then run under identical conditions and a least-squares data-regression approach (24) employed to determine the concentrations of the individual components. Selectivity is based on the difference in phosphorescence lifetimes of the individual components and on any possible wavelength discrimination (21,36).

RESULTS AND DISCUSSION

Phosphorescence Lifetime Determinations. Table I shows the individual phosphorescence lifetimes determined for 10^{-4} M solutions of the seven lumiphores used in this study. Each value is the average of 10 replicate measurements of scattered light and luminescence at a 30-Hz modulation frequency. Two sets of lifetimes are reported in Table I, the first being those determined by the phase-shift approach (Eqn. 1) and the second those determined by demodulation measurements (Eqn. 2).

Several trends can be noted upon close inspection of these results. First, the precision of the phase-shift approach is poorer than that for the demodulation method, mostly because of the difficulties associated with locating the exact maximum of the sine curves stored on the digital oscilloscope. Importantly, we could have employed the lock-in amplifier for for lifetime measurements also; however, we did not because of the

insufficient readability of the lock-in amplifier's phase setting. Second, all except the first-entered sample of p-nitrophenol exhibited simple first-order decays. This first p-nitrophenol sample is clearly heterogeneous (25,16); at least two ground-state populations contribute to its total luminescence, as shown by heterogeneity analysis (25,26) performed at twenty modulation frequencies between 0.5 and 200 Hz. The apparent lifetimes for this sample are 0.400 and 0.035 s, with fractional contributions of 70 and 30%, respectively. It appears that our p-nitrophenol was inadvertently contaminated with m-nitrophenol; a second p-nitrophenol reagent bottle, from the same source, exhibited no similar heterogeneity. Regardless of the source of this heterogeneity, it is evident that the new fiber-optic-based phosphorescence spectrometer is capable of detecting and resolving it.

Elimination of Fluorescence Interference: Detection Limits. Figure 3 shows the phase-resolved emission spectra for individual single-component samples of 10^{-5} M m- and p-nitrophenol in ethanol at 77 K using 30-Hz sinusoidal source modulation. These plots are identical to steady-state spectra (not shown). This similarity indicates that the fluorescence contribution is negligible for these two samples.

In contrast, Figure 4 shows the steady-state and phase-resolved spectra for 10^{-4} M anthracene at 77 K. It is evident that the fluorescence contribution is especially significant below 460 nm in the steady-state scan, but that it can easily be eliminated using phase resolution. Similar results were achieved for the other lumiphores used in this study.

Table II lists the detection limits achieved using the new fiber-optic based phase-resolved phosphorescence spectrometer. These results were derived from phase-resolved measurements at the emission spectral maximum

for a given lumiphore held at 77 K. Detection limits are reported as that concentration of lumiphore required to give a signal (DL) equal to three times the standard deviation for a blank sample. In this study 10 ethanol blanks were run to determine this blank standard deviation. In all cases detection limits are at or below 82 nM.

Binary Mixture Resolution. Several binary mixtures were studies in an attempt to delimit the capabilities of the new fiber-optic-based phosphorimeter. Table III shows the prepared concentrations for binary mixtures of m- and p-nitrophenol (SET I) and for 7,8- and 5,6-benzoquinoline (SET II). Tables IV and V show the statistical information (slope, intercept, correlation coefficient (r), and standard error of estimate (SEE)) taken from plots of the experimentally determined concentrations vs. the actual prepared concentrations (Table III) and as a function of the number of equations employed (number of emission wavelengths).

It is evident that a single pair of emission wavelengths cannot satisfactorily resolve either binary set (Tables IV and V); however, as the number of wavelengths is increased, the information content for the system is increased and better results are obtained. Wavelengths were chosen at evenly spaced intervals about the emission maximum for the mixture spectrum. Not surprisingly, the 7,8- and 5,6-benzoquinoline binary mixtures (Table V) are very difficult to resolve because of their severe spectral overlap and their similar phosphorescence lifetimes (Table I). Again, as the number of wavelengths is increased, the results show significant improvement.

Figures 5 and 6 show three-dimensional data sets of the phase-resolved phosphorescence intensity (PRPI) vs. detector phase angle setting vs. emission wavelength for 1 μM m- and p-nitrophenol, respectively. These data

were collected using approximately 55 mW of laser power through the optical-fiber sensor; data collection time was less than 10 minutes for each set. As discussed by others (21,35,36) the information content of such data sets is quite high and can be used for multicomponent analysis.

Ternary Mixture Resolution. In an effort to more thoroughly evaluate the new fiber-optic-based spectrometer, ternary mixtures of anthracene, phenazine, and acridine were prepared (Table VI). Table VII compiles the statistical information for plots of the experimentally determined concentrations vs. the true concentrations shown in Table VI. As with the binary systems, a single three-wavelength measurement is unable to resolve the three components successfully. As the number of wavelengths is increased, the results improve (SEE decreases and r approaches unity); at twelve wavelengths the results are quite satisfactory.

In all cases (binary and ternary mixtures), a single set of two- or three-wavelength measurements was unable to resolve the individual components. Instead, the number of emission wavelengths had to be increased beyond the number of sample constituents. This finding implies that the phase-resolved phosphorescence intensities at different emission wavelengths are probably correlated. That is, the two or three simultaneous equations that were used are not linearly independent. Fortunately, by increasing the number of emission wavelengths (overdetermining the system) we can apparently generate linearly independent relationships. Another explanation for this situation might be the presence of other "principal components" such as instrument noise and sample-preparation variations. These components would require additional equations in order to thoroughly describe the measurement system and effect a mathematical "separation".

CONCLUSION

The new fiber-optic based phosphorescence spectrometer has several advantages over more conventional low-temperature phosphorescence instruments. First, all the problems associated with a Dewar cell (window frosting and cleaning, cryogent bubbling, etc.) are eliminated with the fiber-optic probe. Second, sample throughput is increased by about a factor of two because between sample clean-up is minimized. Third, inexpensive micro vials can be employed as sample containers. Fourth, detection powers are sufficient to allow the sensitive determination of most phosphorescent species. Finally, measurements can be easily performed in remote inaccessible, confined and hostile environments using the fiber-optic probe. Shortcomings of the system include 1) that after about 250 freeze-thaw cycles the glass capillary shattered and 2) detection limits are not as low as can be obtained with direct excitation and observation of phosphorescence. The shattering problem could perhaps be alleviated in the future through use of a quartz or teflon capillary tube. The detection limit problem is intrinsic to fiber-optic sensors and is part of the trade off between detection power and remote sensing capabilities.

CREDIT

Supported in part by the Office of Naval Research, The Upjohn Co., and the National Science Foundation through grant CHE 83-20053. The authors would also like to thank Dean Gerachi of Galileo Fiber Optics, Inc. for providing the UV-grade fibers.

LITERATURE CITED

1) Wiedmann, E. Ann. Physik 1888, 34, 446.

2) Lewis, G. N. and Kasha, M. J. Amer. Chem. Soc. 1944, 66, 2100.

3) Keirs, R. J., Britt, R. D. and Wentworth, W. E. Anal. Chem. 1957, 29, 202.

4) St. John, P. A. and Winefordner, J. D. Anal. Chem. 1967, 39, 500.

5) Hollifield, J. C. and Winefordner, J. D. Chem. Instrum. 1969, 1, 341.

6) O'Haver, T. C. and Winefordner, J. D. Anal. Chem. 1966, 38, 602.

7) O'Haver, T. C. and Winefordner, J. D. Anal. Chem. 1966, 38, 1258.

8) Winefordner, J. D. Accts. Chem. Res. 1969, 2, 361.

9) Fisher, R. P. and Winefordner, J. D. Anal. Chem. 1972, 44, 948.

10) O'Donnell, C. M., Harbaugh, K. F. and Winefordner, J. D. Anal. Chem. 1972, 45, 381.

11) Gaviola, E. Z. Phys. 1927, 42, 853.

12) Veselova, T. V., Cherkasov, A. S. and Shirokov, V. I. Opt. Spectrosc. 1970, 29, 617.

13) Mousa, J. J. and Winefordner, J. D. Anal. Chem. 1974, 46, 1195.

14) Bright, F. V. and McGown, L. B. Anal. Chim. Acta 1984, 162, 275.

15) McGown, L. B. and Bright, F. V. Anal. Chem. 1984, 56, 2195.

16) Bright, F. V. and McGown, L. B. Talanta 1985, 32, 15.

17) McGown, L. B. and Bright, F. V. Anal. Chim. Acta 1985, 169, 117.

18) Bright, F. V. and McGown, L. B. Anal. Chem. 1985, 57, 55.

19) Bright, F. V. and McGown, L. B. Anal. Chem. 1985, 57, 2877.

20) Bright, F. V., Keimig, T. L. and McGown, L. B. Anal. Chim. Acta 1985, 175, 189.

21) McGown, L. B. and Bright, F. V. Anal. Chem. 1984, 56, 1400A.

22) Nithipatikom, K. and McGown, L. B. Anal. Chem. 1986, 58, 2469.

23) Heiman, D., Rev. Sci. Instrum. 1985, 56, 684.

24) Bright, F. V., Ph.D. Dissertation, Oklahoma State University, 1985.

25) Bright, F. V., Wilson, D. A. and Hieftje, G. M. Appl. Spectrosc. 1986, 40, 683.

26) Bright, F. V., Monnig, C. A. and Hieftje, G. M. Anal. Chem. 1986, 58, 3139.

27) Bright, F. V. and Hieftje, G. M. Appl. Optics, submitted for publication.

28) Hieftje, G. M., Haugen, G. R. and Ramsey, J. M. Appl. Phys. Lett. 1977, 30, 463.

29) Gratton, E. and Limkeman, M. Biophys. J. 1983, 44, 315.

30) Gratton, E. and Barbieri, B. Spectroscopy 1986, 1(6), 28.

31) Winefordner, J. D. and Tin, M. Anal. Chim. Acta 1964, 31, 239.

32) Bauer, R. K. and Balter, A. Opt. Commun. 1979, 28, 91.

33) Weber, G. J. Phys. Chem. 1980, 85, 949.

34) Jameson, D. M., Gratton, E. and Hall, R. D. Appl. Spectrosc. Rev. 1984, 20, 55.

35) Keating-Nakamoto, S. M., Cherek, H. and Lakowicz, J. R. Anal. Chem. 1987, 59, 271.

36) Warner, I. M., Patonay, G. and Thomas, M. P. Anal. Chem. 1985, 57, 463A.

37) McGlynn, S. P., Padhye, M. R. and Kasha, M. J. Chem. Phys. 1955, 23, 593.

38) Moya, H. A. and Winefordner, J. D. J. Arg. Food Chem. 1965, 13, 516.

39) Craig, D. P. and Ross, J. G. J. Chem. Soc. 1954, 1589.

40) Hood, L. V. S. and Winefordner, J. D. Anal. Chem. 1966, 38, 1922.

TABLE I

Measured Phosphorescence Lifetimes (s) of Individual Components.[a] All determined as 10^{-4} M in ethanol at 77 K.

Sample	phase shift method (eq. 1)	demodulation method (eq. 2)	Literature Value	Heterogeneous
Anthracene	0.094(0.013)	0.096(0.008)	0.09[b]	NO
Phenazine	0.321(0.007)	0.317(0.002)	-	NO
Acridine	0.012(0.006)	0.013(0.004)	-	NO
p-nitrophenol[c]	0.314(0.009)	0.389(0.004)	>0.20[d]	YES[e]
p-nitrophenol[c]	0.421(0.016)	0.417(0.007)	>0.20[d]	NO
m-nitrophenol	0.023(0.005)	0.029(0.001)	-	NO
7,8-BQ[f]	1.412(0.019)	1.422(0.001)	1.4-2.1[g]	NO
5,6-BQ[f]	1.882(0.021)	1.890(0.001)	1.8-2.6[g]	NO

[a] values in parentheses are the respective standard deviations for 10 measurements.

[b] reference 37.

[c] samples of p-nitrophenol taken from a contaminated (upper entry) and uncontaminated (lower entry) vessel.

[d] reference 38.

[e] this sample was found to contain both m-and p-nitrophenol. Heterogeneity is indicated by a lack of agreement between phase shift and demodulation lifetimes.

[f] 7,8- and 5,6-BQ represent 7,8- and 5,6-benzoquinoline, respectively.

[g] reference 39.

TABLE II

Detection Limits Obtained with the New Phase-Resolved Phosphorimeter

Sample	Detection Limits (nM)	Literature Values (nM)[a]
Anthracence	182	337[b]
Phenazine	53	-
Acridine	238	-
p-nitrophenol	34	0.02[c]
m-nitrophenol	61	-
7,8 BQ	39	-
5,5 BQ	26	-

7,8- and 5,6-BQ represent 7,8- and 5,6-benzoquinoline.

[a]values are for nonlaser excitation with conventional optical systems.

[b]reference 40.

[c]reference 38.

TABLE III

Constituent Concentrations of Prepared Binary Mixtures of Lumiphores[a] in Ethanol

	SET I		SET II	
Solution	m-nitrophenol	p-nitrophenol	7,8-BQ	5,6-BQ
1	103	131	201	216
2	103	61	201	108
3	50	131	100	216
4	10.3	131	20.1	216
5	10.3	13.1	201	21.6
6	1.03	1.31	2.01	2.16
7	1.03	13.1	2.01	21.6
8	10.3	0.131	20.1	2.16
9	0.103	0.131	0.201	0.216

[a] $\mu\underline{M}$ in micro vial.

5.6- and 7,8-BQ represent 5,6- and 7-8-benzoquinoline.

TABLE IV

Statistical Information for Correlation Plots Between the Determined and Prepared Concentrations for Binary Sample Containing m- and p-Nitrophenol

	# of Eqns.	Slope	Intercept	r	SEE
m-nitrophenol	2	0.923	0.023	0.9347	0.42
p-nitrophenol	2	0.917	0.046	0.9631	0.39
m-nitrophenol	4	0.946	0.017	0.9531	0.27
p-nitrophenol	4	0.971	0.020	0.9726	0.20
m-nitrophenol	6	0.983	0.013	0.9738	0.20
p-nitrophenol	6	0.990	0.010	0.9872	0.18
m-nitrophenol	8	0.993	0.003	0.9924	0.18
p-nitrophenol	8	0.997	0.007	0.9963	0.16

2 Eqns. - Emission at 520 and 530 nm.

4 Eqns. - Emission at 510, 520, 530 and 540 nm.

6 Eqns. - Emission at 510, 515, 520, 530, 535, 540 nm.

8 Eqns. - Emission at 510,515, 520, 525, 530, 535, 540, 545 nm.

SEE - standard error of estimate.

TABLE V

Statistical Information for Correlation Plots Between the Determined and Prepared Concentrations for Binary Samples Containing 7,8- and 5,6-Benzoquinoline

	# of Eqns.	Slope	Intercept	r	SEE
7,8-BQ	2	0.813	0.124	0.7632	1.03
5,6-BQ	2	1.24	0.026	0.8721	1.21
7,8-BQ	4	0.842	0.097	0.7984	0.94
5,6-BQ	4	1.09	0.042	0.8992	1.02
7,8-BQ	6	0.830	0.082	0.8435	0.84
5,6-BQ	6	1.13	0.046	0.9123	0.95
7,8-BQ	8	0.901	0.063	0.8631	0.81
5,6-BQ	8	1.077	0.040	0.9444	0.86
7,8-BQ	All	0.926	0.028	0.9385	0.71
5,6-BQ	All	0.978	0.031	0.9687	0.63

2 Eqns. - Emission at 550 and 560 nm.

4 Eqns. - Emission at 530, 540, 560 and 580 nm.

6 Eqns. - Emission at 530, 535, 540, 550, 555 and 560 nm.

8 Eqns. - Emission at 530, 535, 550, 555, 560, 565, 570 and 575 nm.

All - emission at 2 nm intervals between 530 and 580 nm.

SEE - standard error of estimate.

TABLE VI

Concentrations of the Three Lumiphores Used in Prepared Ternary Samples[a]

Solution	Anthracence	Phenazine	Acridine
1	100	100	100
2	50.0	100	100
3	100	50.0	100
4	100	100	50.0
5	10.0	100	100
6	100	10.0	100
7	100	100	10.0
8	33.3	100	100
9	100	33.3	100
10	100	100	33.3
11	1.00	1.00	1.00
12	0.50	0.50	0.50

[a] μM in micro vial.

TABLE VII

Statistical Information for Correlation Plots Between the Determined and Prepared Concentrations for Ternary Samples Containing Anthracence, Phenazine, and Acridine

	# of Eqns.	Slope	Intercept	r	SEE
Anthracene	3	0.863	0.023	0.9013	2.00
Phenazine	3	0.914	0.036	0.9047	0.91
Acridine	3	0.921	0.020	0.9325	0.93
Anthracene	6	0.871	0.020	0.9537	1.80
Phenazine	6	0.927	0.031	0.9423	0.83
Acridine	6	0.941	0.027	0.9704	0.65
Anthracene	9	0.913	0.017	0.9631	1.60
Phenazine	9	0.971	0.030	0.9725	0.81
Acridine	9	0.934	0.013	0.9847	0.60
Anthracene	12	0.925	0.009	0.9704	1.50
Phenazine	12	0.981	0.016	0.9781	0.70
Acridine	12	0.937	0.004	0.9853	0.59

3 Eqns. - Emission at 3 equally spaced wavelengths between 500 and 580 nm.

6 Eqns. - Emission at 6 equally spaced wavelengths between 500 and 580 nm.

9 Eqns. - Emission at 9 equally spaced wavelengths between 500 and 580 nm.

12 Eqns. - Emission at 12 equally spaced wavelengths between 500 and 580 nm.

SEE - standard error of estimate.

FIGURE CAPTIONS

Figure 1. Schematic diagram of the new fiber-optic based phase-resolved phosphorescence spectrometer. Abbreviations are M_1 and M_2, mirrors; L_1 and L_2, lenses; x,y,z, x,y,z-translation stage; OFS, optical-fiber sensor; PMT, photomultiplier tube; FM, fiber mount.

Figure 2. Diagram of the low-temperature phosphorescence fiber-optic sampling system.

Figure 3. Phase-resolved phosphorescence spectra for m- and p-nitrophenol in ethanol at 77 K. Modulation frequency 30 Hz. Scan time 6 minutes.

Figure 4. Steady-state and phase-resolved phosphorescence spectra for anthracene in ethanol at 77 K. Modulation frequency 30 Hz. Scan time 6 minutes.

Figure 5. Three-dimensional data set of phase-resolved phosphorescence intensity (PRPI) vs. detector phase angle vs. emission wavelength for 1 μM m-nitrophenol. Modulation frequency is 50 Hz.

Figure 6. Three-dimensional data set of phase-resolved phosphorescence intensity (PRPI) vs. detector phase angle vs. emission wavelength for 1 μM p-nitrophenol. Modulation frequency is 50 Hz.

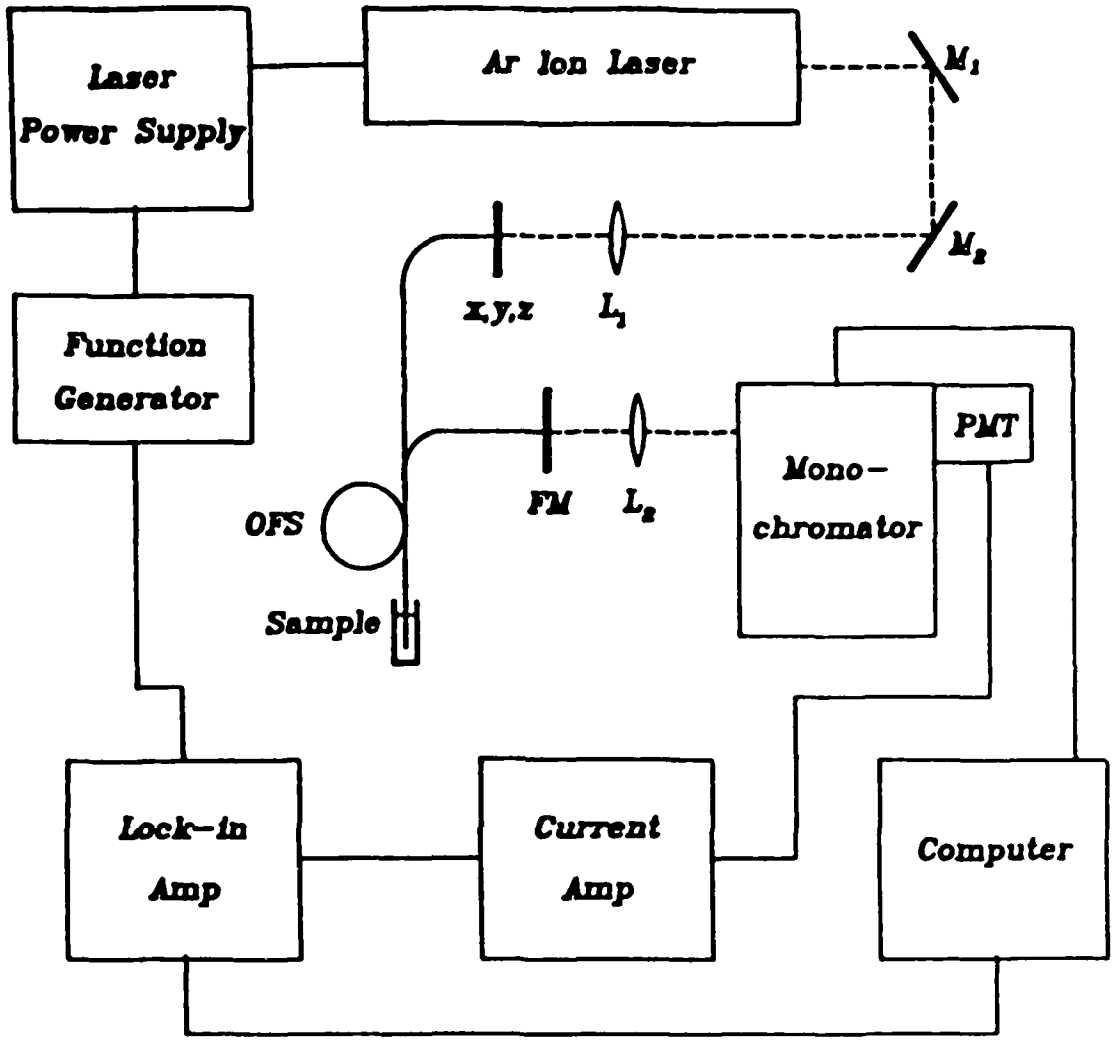
Laser
Power Supply
Ar Ion Laser
M_1
M_2
x,y,z
L_1
Function
Generator
PMT
Mono-
chromator
FM
L_2
OFS
Sample
Lock-in
Amp
Current
Amp
Computer

Fig 1

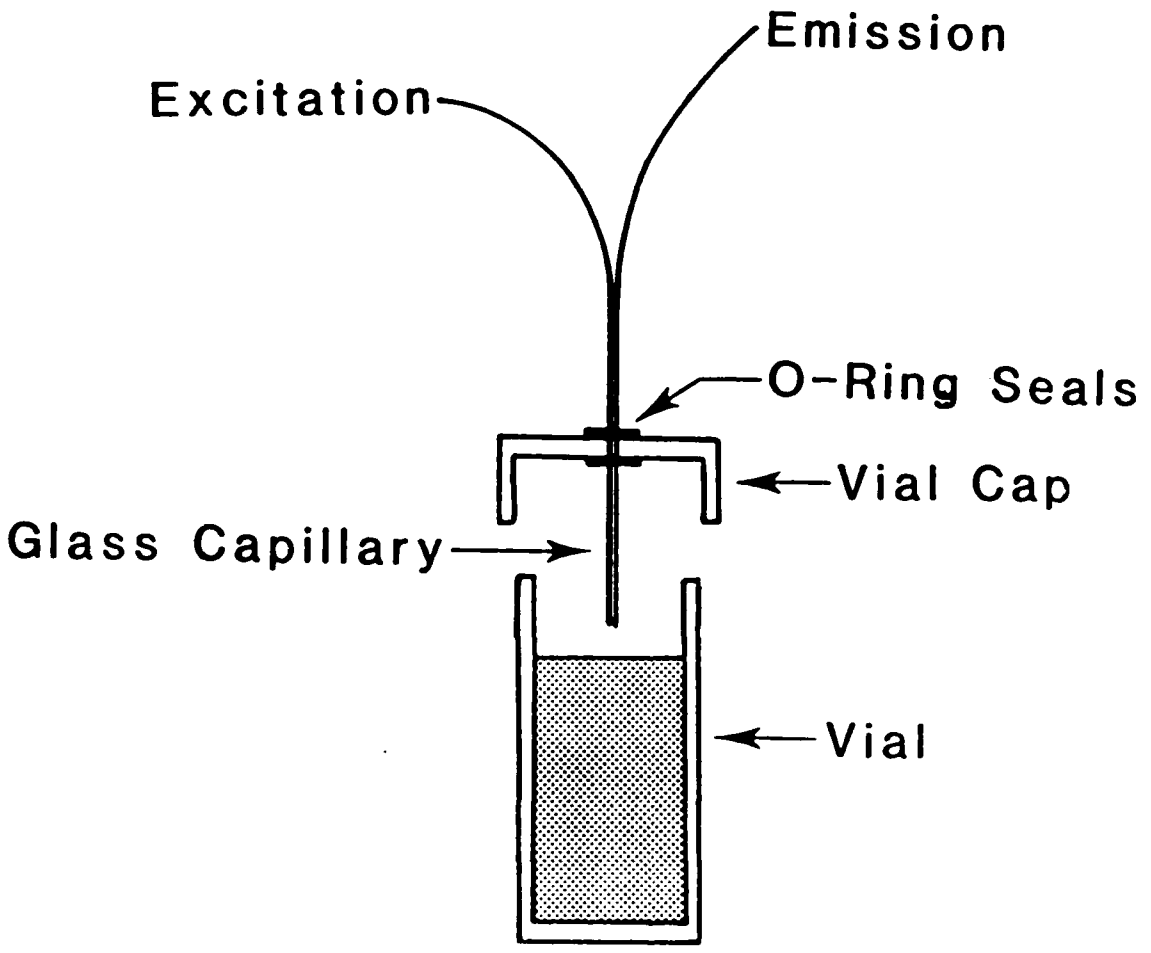
Emission
Excitation
O-Ring Seals
Vial Cap
Glass Capillary
Vial

Fig. 2

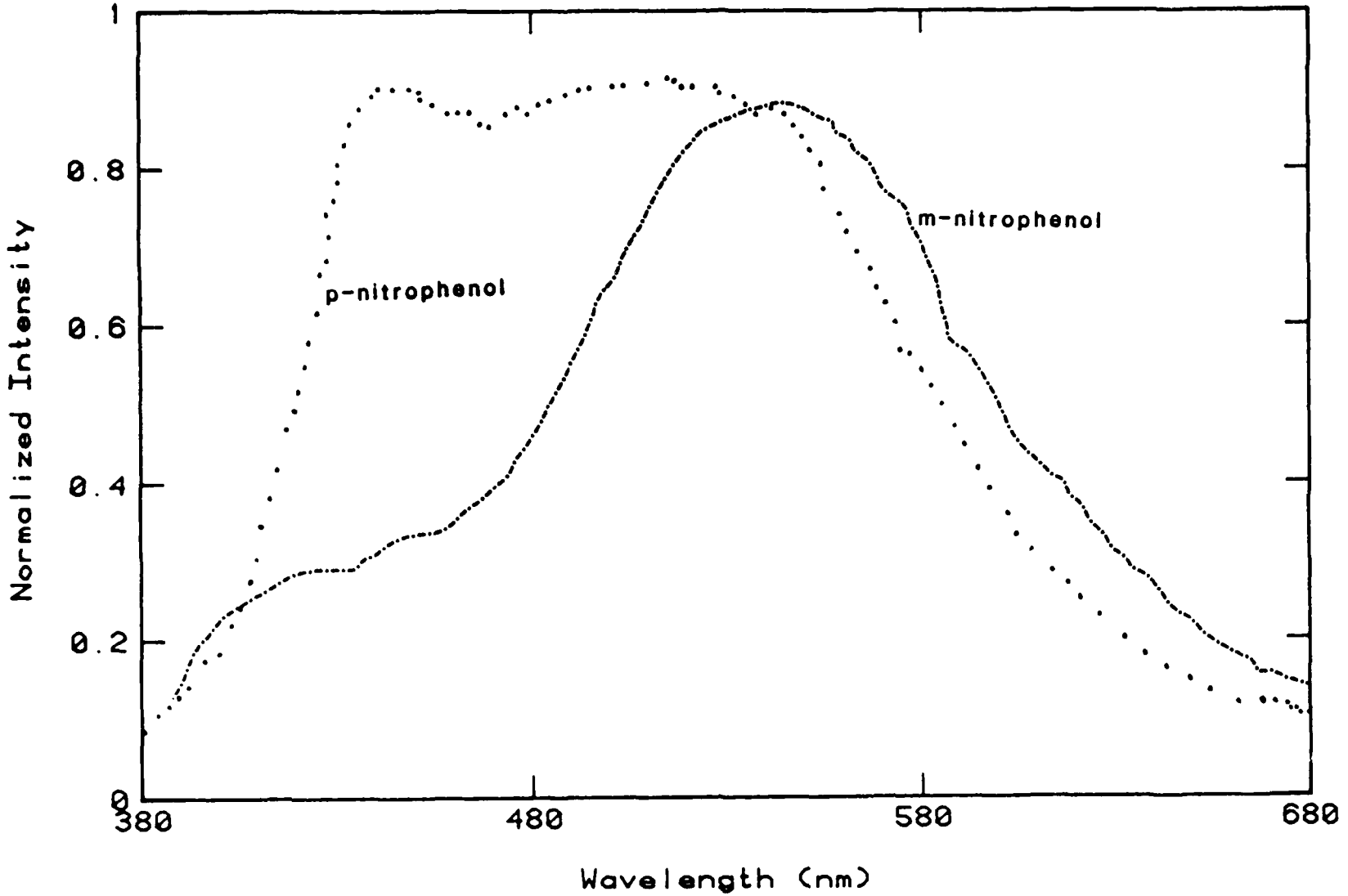
1
0.8
0.6
0.4
0.2
0
Normalized Intensity
p-nitrophenol
m-nitrophenol
380
480
580
680
Wavelength (nm)

Fig. 3

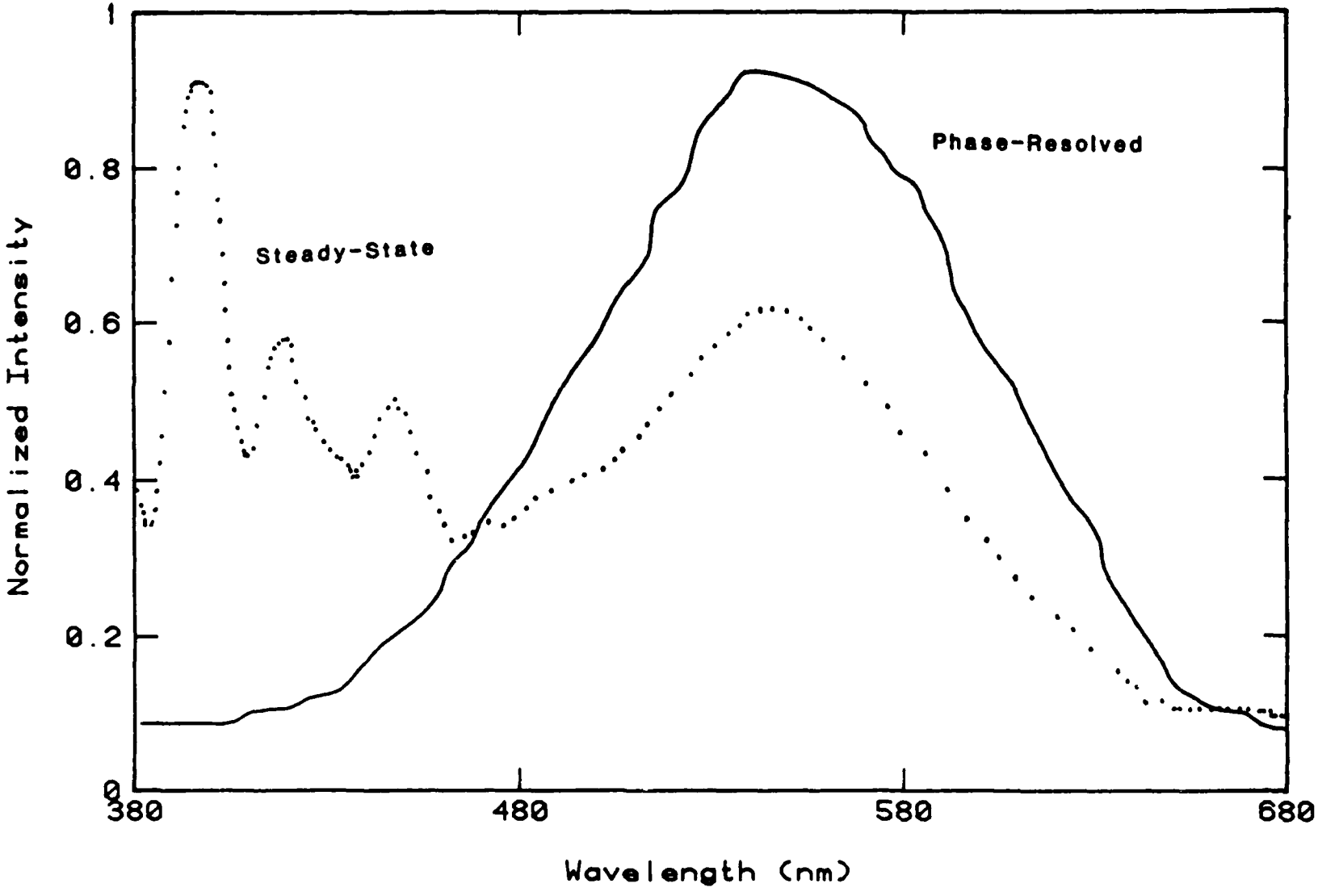
Normalized Intensity
1
0.8
0.6
0.4
0.2
0
380
480
580
680
Wavelength (nm)
Steady-State
Phase-Resolved

Fig. 4

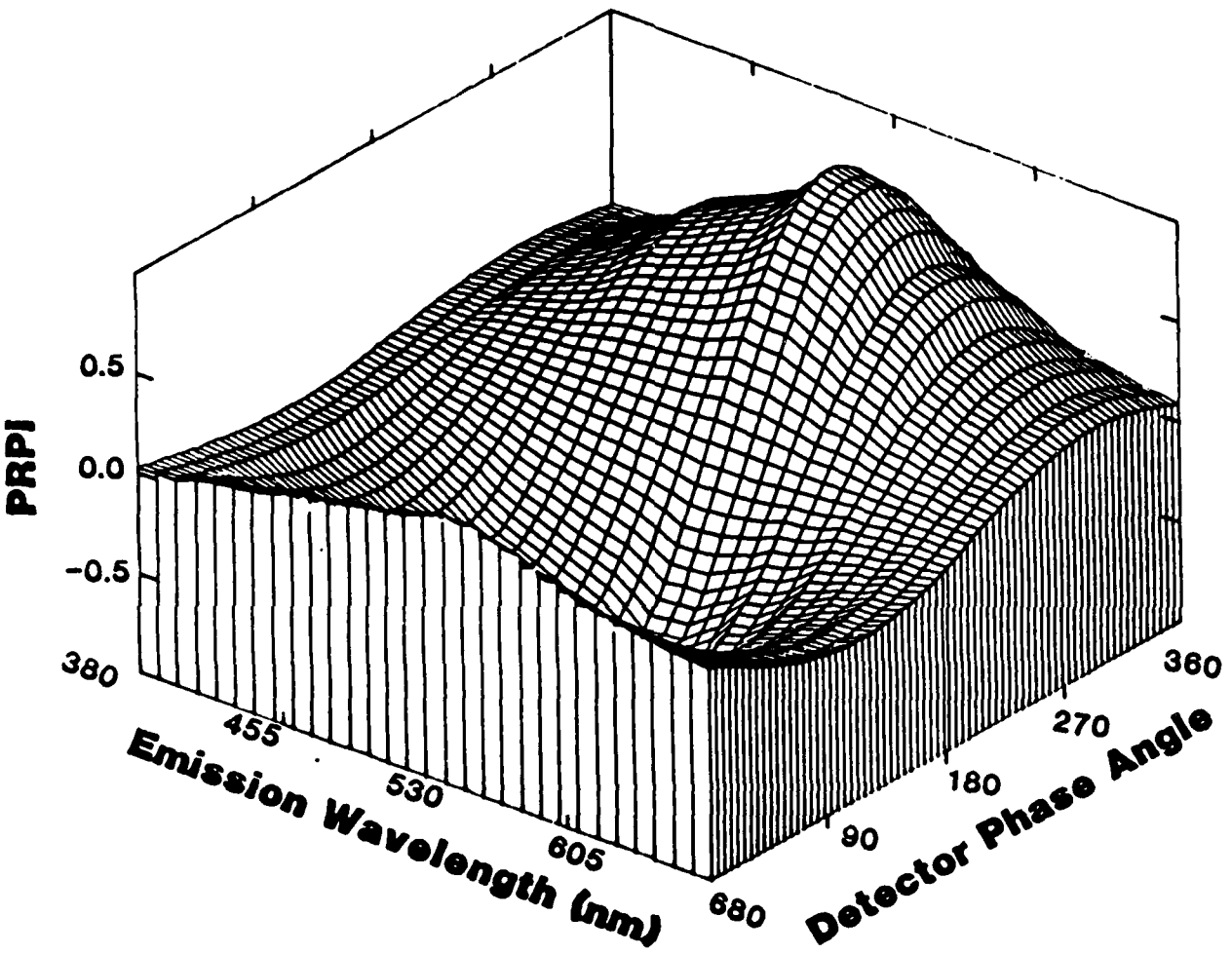
PRPI
0.5
0.0
-0.5
380
455
530
605
680
Emission Wavelength (nm)
90
180
270
360
Detector Phase Angle

Fig. 5

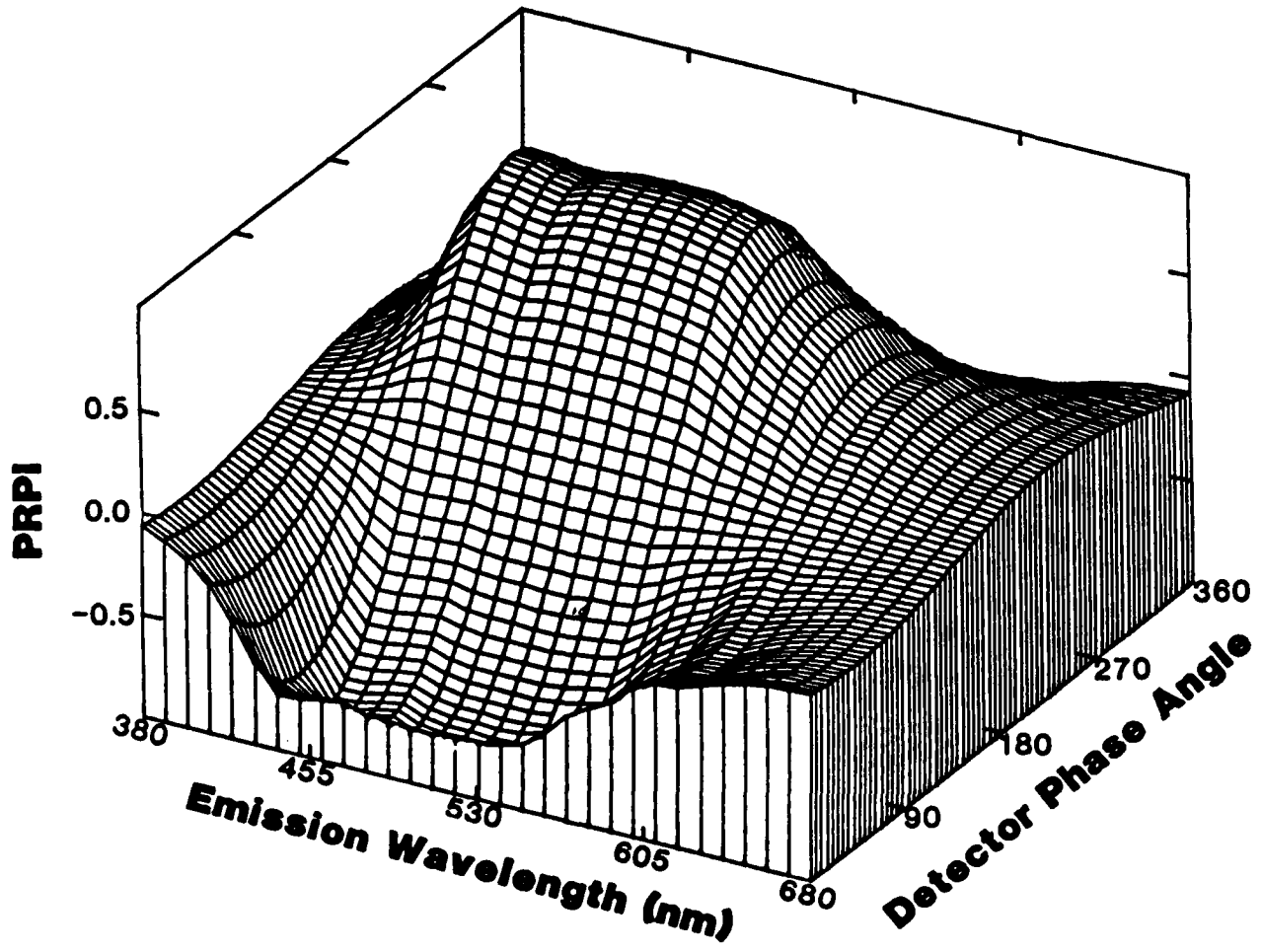
PRPI
0.5
0.0
-0.5
380
455
530
605
680
Emission Wavelength (nm)
90
180
270
360
Detector Phase Angle

Fig. 6

TECHNICAL REPORT DISTRIBUTION LIST, GEN

	No. Copies
Office of Naval Research Attn: Code 1113 800 N. Quincy Street Arlington, Virginia 22217-5000	2
Dr. Bernard Douda Naval Weapons Support Center Code 50C Crane, Indiana 47522-5050	1
Naval Civil Engineering Laboratory Attn: Dr. R. W. Drisko, Code L52 Port Hueneme, California 93401	1
Defense Technical Information Center Building 5, Cameron Station Alexandria, Virginia 22314	12 high quality
DTNSRDC Attn: Dr. H. Singerman Applied Chemistry Division Annapolis, Maryland 21401	1
Dr. William Tolles Superintendent Chemistry Division, Code 6100 Naval Research Laboratory Washington, D.C. 20375-5000	1
Dr. David Young Code 334 NORDA NSTL, Mississippi 39529	1
Naval Weapons Center Attn: Dr. Ron Atkins Chemistry Division China Lake, California 93555	1
Scientific Advisor Commandant of the Marine Corps Code RD-1 Washington, D.C. 20380	1
U.S. Army Research Office Attn: CRD-AA-IP P.O. Box 12211 Research Triangle Park, NC 27709	1
Mr. John Boyle Materials Branch Naval Ship Engineering Center Philadelphia, Pennsylvania 19112	1
Naval Ocean Systems Center Attn: Dr. S. Yamamoto Marine Sciences Division San Diego, California 91232	1

END

DATE

FILMED

5-88

DTIC